17. Crevier, D. W. & Meister, M. Synchronous period-doubling in flicker vision of salamander and man. *J. Neurophysiol.* **79,** 1869–1878 (1998).
18. Merigan, W. H. & Maunsell, J. H. How parallel are the primate visual pathways? *Annu. Rev. Neurosci.* **16,** 369–402 (1993).
19. Sparks, D. L. Translation of sensory signals into commands for control of saccadic eye movements: role of primate superior colliculus. *Physiol. Rev.* **66,** 118–171 (1986).
20. Knudsen, E. I. Auditory and visual maps of space in the optic tectum of the owl. *J. Neurosci.* **2,** 1177–1194 (1982).
21. Corey, D. P. & Hudspeth, A. J. Response latency of vertebrate hair cells. *Biophys. J.* **26,** 499–506 (1979).
22. Carandini, M., Heeger, D. J. & Movshon, J. A. Linearity and normalization in simple cells of the macaque primary visual cortex. *J. Neurosci.* **17,** 8621–8644 (1997).
23. Abbott, L. F., Varela, J. A., Sen, K. & Nelson, S. B. Synaptic depression and cortical gain control. *Science* **275,** 220–224 (1997).
24. Knudsen, E. I., du Lac, S. & Esterly, S. D. Computational maps in the brain. *Annu. Rev. Neurosci.* **10,** 41–65 (1987).
25. Meister, M., Pine, J. & Baylor, D. A. Multi-neuronal signals from the retina: acquisition and analysis. *J. Neurosci. Methods* **51,** 95–106 (1994).
26. Hunter, I. W. & Korenberg, M. J. The identification of nonlinear biological systems: Wiener and Hammerstein cascade models. *Biol. Cybern.* **55,** 135–144 (1986).
27. Rodieck, R. W. Quantitative analysis of cat retinal ganglion cell response to visual stimuli. *Vision Res.* **5,** 583–601 (1965).
28. Warland, D. K., Reinagel, P. & Meister, M. Decoding visual information from a population of retinal ganglion cells. *J. Neurophysiol.* **78,** 2336–2350 (1997).
29. Devries, S. H. & Baylor, D. A. Mosaic arrangement of ganglion cell receptive fields in rabbit retina. *J. Neurophysiol.* **78,** 2048–2060 (1997).

Acknowledgements. We thank J. Keat for assistance in generating the visual stimulus, and H. Berg and T. Holy for comments on the manuscript. This work was supported by a NRSA to M.B. and a grant from the NIH and a Presidential Faculty Fellowship to M.M.

Correspondence and requests for material should be addressed to M.J.B. (e-mail: berry@biosun.harvard.edu).

A new cellular mechanism for coupling inputs arriving at different cortical layers

Matthew E. Larkum, J. Julius Zhu & Bert Sakmann

Abt. Zellphysiologie, Max-Planck-Institut für Medizinische Forschung, Jahnstrasse 29, D-69120 Heidelberg, Germany

Pyramidal neurons in layer 5 of the neocortex of the brain extend their axons and dendrites into all layers. They are also unusual in having both an axonal and a dendritic zone for the initiation of action potentials[1–6]. Distal dendritic inputs, which normally appear greatly attenuated at the axon, must cross a high threshold at the dendritic initiation zone to evoke calcium action potentials[1,7] but can then generate bursts of axonal action potentials. Here we show that a single back-propagating sodium action potential generated in the axon[8] facilitates the initiation of these calcium action potentials when it coincides with distal dendritic input within a time window of several milliseconds. Inhibitory dendritic input can selectively block the initiation of dendritic calcium action potentials, preventing bursts of axonal action potentials. Thus, excitatory and inhibitory postsynaptic potentials arising in the distal dendrites can exert significantly greater control over action potential initiation in the axon than would be expected from their electrotonically isolated locations. The coincidence of a single back-propagating action potential with a subthreshold distal excitatory postsynaptic potential to evoke a burst of axonal action potentials represents a new mechanism by which the main cortical output neurons can associate inputs arriving at different cortical layers.

Triple recordings were made on two sites of the apical dendrites and the somata of layer-5 pyramidal neurons (Fig. 1a). Subthreshold excitatory-postsynaptic-potential(EPSP)-shaped potentials in the distal apical dendrites were strongly attenuated as they spread to the soma (Fig. 1b). Back-propagating action potentials from the axon reached the distal dendritic tufts (Fig. 1c) where they caused an influx[9] of Ca^{2+}. However, single sodium action potentials (Na^+-APs) initiated in the axon do not evoke a calcium action potential (Ca^{2+}-AP) in the dendrite[1,3,4,6–9] (Fig. 1c). The combination of a subthreshold EPSP-shaped distal dendritic potential (Fig. 1b) and a back-propagating action potential (Fig. 1c) elicited a Ca^{2+} and Na^+ action potential complex in the dendrite (Fig. 1d; $n = 27$) that resulted in 2–3 (2.2 ± 0.1; frequency: 101 ± 8 Hz) Na^+-APs at the soma. This back-propagating action potential activated Ca^{2+} spike firing (BAC firing) was evoked with 1.1 nA (± 0.1 nA) peak current injection at a distal dendritic location (average 693 ± 18 μm from soma). This was only half the current amplitude ($49 \pm 4\%$; $n = 27$) that evoked a comparable Ca^{2+}-AP in the absence of a back-propagating action potential (Fig. 1e). In the neuron shown in Fig. 1d, the current needed was only 0.3 nA (25% of threshold). The threshold dendritic current for BAC firing was typically less than the threshold for eliciting a Na^+-AP using the same-shaped current injection at the soma, suggesting that the dendritic component requires fewer synaptic inputs than are needed for axonal Na^+-APs (possibly less than ten inputs[1]).

The optimal time for eliciting a Ca^{2+}-AP with dendritic current injection was 3–7 ms after the somatic action potential. At threshold, the time interval (Δt) for evoking BAC firing was very narrow. Here, dendritic current injection given at Δt values of 3, 7 and 11 ms (Fig. 2a–c, respectively) elicited BAC firing only at $\Delta t = 7$ ms. The average threshold for BAC firing was measured at 5-ms time intervals (Fig. 2d; $n = 8$) and revealed a sharp minimum at $\Delta t = 5$ ms. The threshold for BAC firing rose sharply for delays of over 5 ms, and was even higher than the threshold for eliciting a Ca^{2+}-AP in the absence of a back-propagating action potential for delays of 10–130 ms. This shows that the generation of a Ca^{2+}-AP is greatly facilitated if the dendritic EPSP and axonal action potential

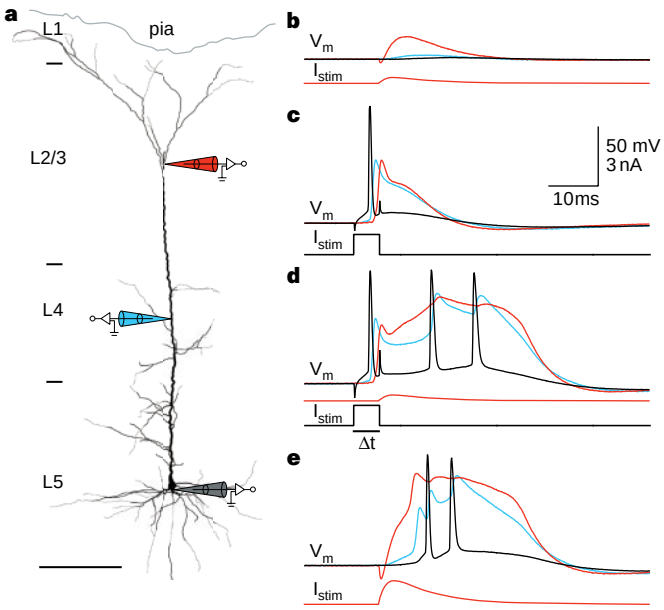

Figure 1 Coupling of a back-propagating action potential (AP) with distal subthreshold current injection. **a**, Reconstruction of a biocytin-filled pyramidal neuron, with the recording pipette positions shown symbolically (770 μm from soma in red, 400 μm from soma in blue and one at the soma in grey). Cortical layers are indicated on the left. Scale bar, 200 μm. **b**, Current injection of 0.3 nA (peak amplitude) at the distal pipette (red trace, bottom) in the shape of an EPSP produced a signal of only 1.4 mV at the soma. It did not reach threshold for either a Ca^{2+}-AP or a Na^+-AP. I_{stim} refers to traces representing current injected and V_m to potential recorded. Positive current causes intracellular depolarization. The colour indicates the corresponding electrode in the diagram. **c**, Threshold current injection at the soma (black trace labelled I_{stim}) evoked an AP that reduced in amplitude but increased in width in the dendrite. **d**, BAC firing. The combination of these injections of current (used in **b** and **c**) separated by an interval (Δt) of 5 ms evoked a burst of APs following the onset of the Ca^{2+}-AP in the distal dendrite. (Δt, time between the onset of each pulse.) Scale bars in **c** also apply to **b** and **d**. **e**, A similar dendritic Ca^{2+}-AP could be evoked by a larger (1.2 nA) current injection alone at the distal dendritic electrode, as shown previously[1].

are timed so that they coincide within a few milliseconds, but is slightly depressed if the EPSP follows a back-propagating action potential 10–130 ms later.

The mechanism underlying the generation of bursts of action potentials is the fact that a Ca^{2+}-AP, once it is elicited in the dendritic initiation zone, can cause enough depolarization at the axonal initiation zone to cross threshold in adult (>P28) rats[7] (Fig. 1e). It gives rise to complex dendritic potentials once threshold has been reached. The back-propagating action potential substantially lowers the threshold for the initiation of this dendritic Ca^{2+}-AP. This event then initiates a burst of axonal action potentials that propagate back into the dendritic arbor. Therefore the final output pattern of the neuron, when combining a back-propagating action potential with a subthreshold EPSP, consists of the first action potential that is generated in the axon, and the second and third action potentials that are an intrinsic property of the neuron for suprathreshold distal dendritic input. This even occurred in cells in which prolonged somatic depolarization did not elicit such a burst pattern. BAC firing was found in all 27 layer-5 pyramidal neurons tested, of which 21 were 'regularly spiking' and 6 were 'intrinsically bursting', as defined by somatic current injection[10].

Extracellularly evoked subthreshold synaptic input (Fig. 3a, b), coupled with a back-propagating action potential, could generate a dendritic Ca^{2+}-AP (in 3 of 10 neurons; Fig. 3c). In most neurons (7 out of 10), the Ca^{2+}-AP was not as large or was non-existent until the addition of low concentrations of GABA antagonists, bicuculline (1 μM) and saclofen (100 μM), which increased the proportion of excitatory to inhibitory input. After application, extracellularly evoked synaptic input coupled with a back-propagating action potential could always evoke a Ca^{2+}-AP in the dendrite ($n = 3/3$). A relatively small extracellularly evoked EPSP was sufficient (an EPSP of 9 mV in the distal dendrite was the smallest needed). Besides showing that synaptic input could generate BAC firing, this experiment also implied that inhibition might selectively modulate the generation of the Ca^{2+}-AP. It is known, for instance, that GABAergic inhibition can affect dendritic Ca^{2+}-APs and Ca^{2+} influx due to back-propagating action potentials in hippocampal pyramidal neurons[11–13].

To test whether GABAergic inhibition affected the Ca^{2+}-AP component of BAC firing, we made simultaneous recordings from interneurons and dendritic and somatic recordings from target pyramidal neurons (Fig. 4a). First, BAC firing was generated in the usual way by coupling a back-propagating action potential with a subthreshold EPSP-shaped dendritic current injection (Fig. 4b). The effect of unitary inhibitory postsynaptic potentials (IPSPs) on the back-propagating action potential itself was small and was only visible when the IPSP and the back-propagating action potential were coincident. In contrast, unitary IPSPs abolished the Ca^{2+}-AP and the associated action potential burst completely (Fig. 4c, recording 1; $n = 5/5$). Trains of presynaptic action potentials in interneurons or long depolarization causing bursts of action potentials could prevent the Ca^{2+}-AP component up to 150 ms in advance (data not shown). By using an extracellular stimulus electrode positioned within 500 μm from the pyramidal neuron and by blocking excitatory transmission with 20 μM CNQX and 50 μM AP5, BAC firing was blocked up to 400 ms in advance ($n = 14$; data not shown).

The action of inhibition was located at the dendritic initiation zone. This was concluded from experiments in which the Ca^{2+}-AP was isolated from the soma. In six experiments, the Ca^{2+}-AP component of BAC firing did not generate a burst of Na^{+}-APs at the soma. The Ca^{2+}-AP could also be isolated with hyperpolarizing

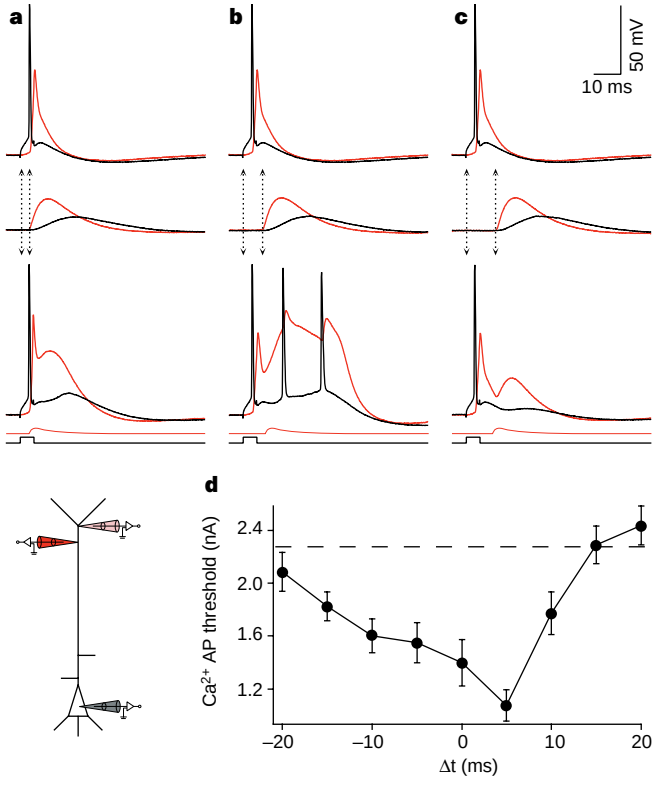

Figure 2 Precision of timing required. Experimental configuration shown diagrammatically (lower left). Recordings were made from the dendrite (red; 600 μm from the soma) and the soma (black) of a L5 pyramidal neuron. A third dendritic electrode (pink; 700 μm from the soma) was used for injecting current. (Electrode colours correspond to recording traces.) Time intervals (**a**, 3 ms; **b**, 7 ms; and **c**, 11 ms) elicited a burst of APs only in **b** at threshold. Δt was taken as the time between the start of the somatic current injection and that of the dendritic current injection. Note, however, that the AP due to the somatic current injection followed the onset by ~3 ms in this case. **d**, A burst of APs could be generated by the combination of dendritic current injection and a back-propagating AP at other times, but the threshold for this was least at $\Delta t = 5$ ms. Each point is the average of 8 neurons (error bars, s.e.m.) and represents the threshold for current injection needed to elicit a dendritic Ca^{2+}-AP. Dashed line represents the Ca^{2+}-AP threshold without a back-propagating AP (2.28 ± 0.14 nA). For ~100 ms after $\Delta t = 10$ ms, the threshold was even slightly higher than without the back-propagating AP.

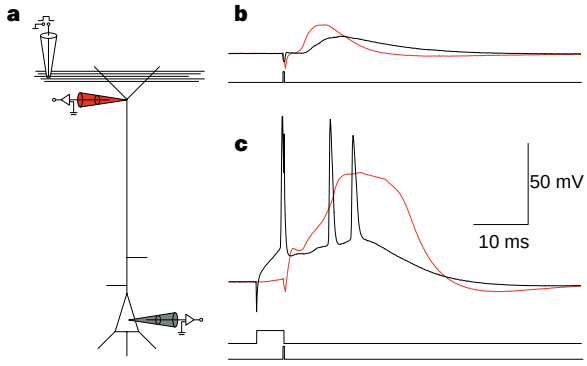

Figure 3 Extracellularly evoked BAC-firing. **a**, Experimental configuration. A bipolar electrode was placed over the layer-1 fibres ~500 μm from the pyramidal cell. **b**, Subthreshold extracellular stimulus of 5 V evoked an EPSP of 17.5 mV in the tufts of a L5 pyramidal neurons (800 μm from the soma; red) and 10 mV at the soma (black). Here the extracellular stimulus presumably evoked synaptic inputs arising mostly in the distal dendrites but also partly near the soma, judging from the small difference in amplitudes at both electrodes. **c**, By preceding the extracellular stimulus with a back-propagating AP ($\Delta t = 5$ ms), a Ca^{2+}-AP was evoked that was similar to the Ca^{2+}-AP evoked with direct dendritic current injection and a back-propagating AP in the same neuron. (Timing and shape of current injections shown below voltage recordings; red for the dendritic electrode and black for the somatic electrode.)

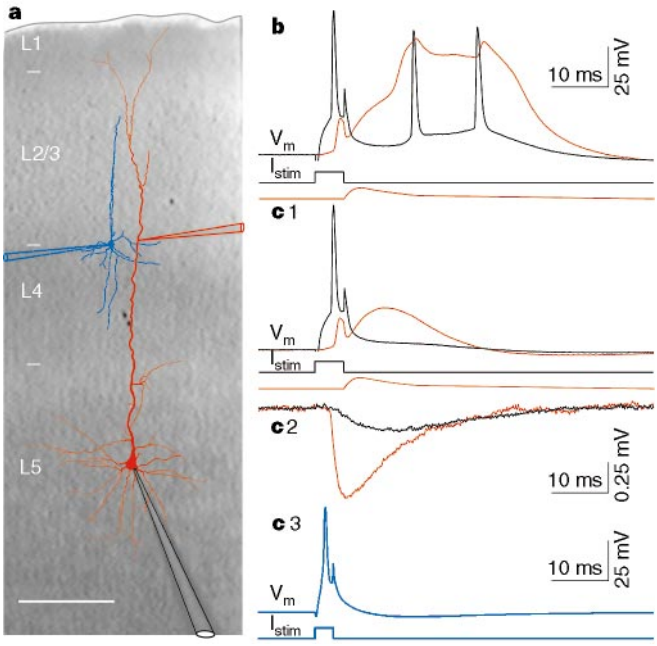

Figure 4 Inhibition of BAC firing. **a**, Reconstruction of the dendritic arbor of a biocytin-filled pyramidal neuron (red neuron) and an inhibitory neuron connected to it (blue neuron) superimposed on a phase-contrast image taken during the experiment showing the cortical layers (labels in white). Pipette positions on the dendrite (red, 550 μm from soma), soma (black) and on the presynaptic neuron (blue) are superimposed symbolically. Scale bar, 200 μm. **b**, BAC firing. Threshold was 0.7 nA when injected through the dendritic pipette 5 ms after the start of injection of current at the soma. **c**, Recordings: 1, unitary inhibitory input blocked the burst of APs but not the somatic AP; 2, the IPSP evoked by a single presynaptic AP was larger at the dendritic electrode (–0.75 mV) than at the soma (–0.2 mV); 3, AP in the presynaptic inhibitory neuron that was responsible for the unitary IPSP shown in recording 2.

current injected at the soma ($n = 2$) or by using shorter dendritic current injections (time to peak 0.1–3.2 ms; $n = 16$). In such conditions, the effect of inhibition, which abolished the isolated Ca^{2+}-AP but not the back-propagating Na^{+}-AP, must have been on the dendritic initiation zone. Moreover, Ca^{2+}-APs evoked by suprathreshold dendritic depolarization could be blocked up to 400 ms in advance ($n = 28$; data not shown) by extracellularly evoked inhibition in the presence of 50 μM AP5 and 20 μM CNQX. Hyperpolarizing or depolarizing the dendrite and/or soma immediately preceding the generation of a Ca^{2+}-AP had no effect on the threshold for evoking Ca^{2+}-APs, indicating that the action of the inhibition was not mediated through a voltage-dependent mechanism. We suggest that the mechanism might be due to shunt by $GABA_A$ and $GABA_B$ conductances and may also involve the activation or inactivation of dendritic conductances[14].

The time-sensitive coupling of a back-propagating action potential with distal excitatory input in L5 pyramidal neurons suggests a new mechanism by which neocortical pyramidal neurons can associate synaptic inputs arriving in the upper and lower layers within a few milliseconds. Which particular input pathways might be associated will depend on the local cortical architecture and is likely to vary in different areas of the cortex. At the cellular level, the mechanism itself appears to be very robust (observed in all 27 L5 pyramidal neurons tested). It involves the co-activation of two initiation zones, which only occurs with specific spatial and temporal input.

Thus, BAC firing provides a potential mechanism for binding different cortical regions[15]. For example, it has been suggested that temporal binding occurs as a result of coincident activation of specific thalamic input to layer 4 and nonspecific thalamic input to layers 1 and 2 (ref. 16). Absence of such nonspecific input is accompanied by cortical dysfunction[17]. Furthermore, extracellular recordings made from the somatosensory cortex of monkeys have shown that natural touch stimulation evokes a fast signal in the lower cortical layers, followed by a slow signal in the upper cortical layers[18]. The slow component was abolished by slow-wave-sleep-induced inhibition.

BAC firing alone would presumably be unstable in an interconnected structure like the cortex and lead to cells continuously bursting in the absence of some other regulatory mechanism. We have shown that inhibition can selectively modulate the ability of the neuron to fire a Ca^{2+}-AP without blocking the generation of Na^{+}-APs due to depolarization at the axonal initiation site. Inhibition, therefore, would act to decouple inputs that would otherwise be associated. Surprisingly, the effect of inhibition appears to last for up to ~400 ms, in contrast to the relatively precise timing of the back-propagating action potential and distal EPSP required for BAC firing to occur. This suggests that inhibition acts as a form of general veto on this kind of burst firing.

Ca^{2+}-APs occur *in vivo* owing to synaptic input[5,12,19,20]. As these Ca^{2+}-APs can cause bursts of action potentials that might signify the association of functionally separated input, it is crucial to understand what sort of postsynaptic effects a burst in L5 pyramidal neurons may have and what sort of information it might encode[21]. Of course, bursts may also occur for reasons other than BAC firing. Our results show that BAC firing could serve as a mechanism for facilitating such spiking behaviour.

In summary, at least two regions of L5 pyramidal neurons can generate action potentials. One has a low threshold and integrates predominantly input at basal and apical oblique dendrites, and the other integrates mostly input that arrives in the distal regions of the apical dendrite. If threshold is reached at the axonal site of integration, the subsequent back-propagating action potential enables threshold at the dendritic initiation site to be reached more easily. Thus, near-synchronous input to both distal and proximal dendrites causes a burst of axonal action potentials, whereas the same-sized input to either region alone does not cause a burst. The complex interaction between the dendritic and axonal initiation sites described here therefore constitutes a new cellular mechanism by which the firing behaviour of output neurons of the cortex can be modulated by synchronous synaptic inputs arriving at different lamina. Furthermore, inhibition can selectively modulate the coupling of the two initiation zones without reducing the ability of the cell to discharge axonal action potentials. □

Methods

Experiments were done in somatosensory neocortical slices from P28–P58 Wistar rats ($n = 57$). Rats were deeply anaesthetized by halothane and decapitated. The brain was quickly removed into cold (0–4 °C) oxygenated physiological solution containing (in mM); NaCl, 125; KCl, 2.5; NaH_2PO_4, 1.25; $NaHCO_3$, 25; $MgCl_2$, 1; dextrose, 25; and $CaCl_2$, 2, pH 7.4. Sagittal slices, 250–300 μm thick, were cut from the tissue blocks with a microslicer and kept at 37 °C.

All experiments were done at 34.0 ± 0.5 °C, with dual and triple recordings from single, identified layer-5 pyramidal neurons using infrared illumination combined with differential interference contrast optics[22]. Somatic (5–10 MΩ) and dendritic (10–25 MΩ) recording pipettes were filled with the standard intracellular solution containing (in mM): potassium gluconate, 115; HEPES, 10; $MgCl_2$, 2; Mg–ATP, 2; Na_2ATP, 2; GTP, 0.3; KCl, 20; and biocytin, 0.25%, pH 7.3. For some recordings, 30 mM KCl and 105 mM potassium gluconate were used. Whole-cell recordings were made with up to three Axoclamp-2B amplifiers (Axon Instruments). Dendritic current injection was made in the shape of a double exponential ($f(t) = (1 - e^{-1/\tau_1}) \times e^{-1/\tau_2}$) with τ_1 being 0.5–2 ms and τ_2, 2–8 ms. The function was adjusted so that the peak current injection corresponded to the value referred to as the amplitude.

Extracellularly evoked synaptic stimulation was induced by a bipolar

electrode with single-voltage pulses (100–200 μs, up to 5 V). The stimulating electrode was typically placed over layer 1 about 500 μm lateral to the cells. After recordings, slices were fixed and stained as described[1]. All results are reported as mean ± s.e.m.

Received 23 October 1998; accepted 25 January 1999.

1. Schiller, J., Schiller, Y., Stuart G. & Sakmann, B. Calcium action potentials restricted to the distal apical dendrites of rat neocortical pyramidal neurons. *J. Physiol.* **505,** 605–616 (1997).
2. Spencer, W. A. & Kandel, E. R. Electrophysiology of hippocampal neurons IV. Fast prepotentials. *J. Neurophys.* **24,** 272–295 (1961).
3. Magee, J., Hoffman, D., Colbert, C. & Johnston, D. Electrical and calcium signaling in dendrites of hippocampal pyramidal neurons. *Annu. Rev. Physiol.* **60,** 327–346 (1998).
4. Kim, H. G. & Connors, B. W. Apical dendrites of the neocortex: correlation between sodium- and calcium-dependent spiking and pyramidal cell morphology. *J. Neurosci.* **13,** 5301–5311 (1993).
5. Hirsch, J. A., Alonso, J. M. & Reid, C. R. Visually evoked calcium action potentials in cat striate cortex. *Nature* **378,** 612–616 (1995).
6. Rhodes, P. A. Functional Implications of Active Currents in the Dendrites of Pyramidal Neurons in *Cerebral Cortex* (eds Ulinski, P. & Jones, E. G.) Vol. 13, 139–200 (Plenum, New York, 1999).
7. Zhu, J. J. & Sakmann, B. Postnatal development of Ca^{2+}-mediated action potentials in dendritic tufts of rat neocortical pyramidal neurons. *Soc. Neurosci. Abstr.* **23,** 2283 (1997).
8. Stuart, G. & Sakmann, B. Active propagation of somatic action potentials into neocortical pyramidal cell dendrites. *Nature* **367,** 69–72 (1994).
9. Markram, H., Helm, P. J. & Sakmann, B. Dendritic calcium transients evoked by single back-propagating action potentials in rat neocortical pyramidal neurons. *J. Physiol (Lond.)* **485,** 1–20 (1995).
10. Connors, B. W. & Gutnick, M. J. Intrinsic firing patterns of diverse neocortical neurons. *Trends Neurosci.* **13,** 99–104 (1990).
11. Miles, R., Toth, K., Gulyas, A. I., Hajos, N. & Freund, T. F. Differences between somatic and dendritic inhibition in the hippocampus. *Neuron* **16,** 815–823 (1996).
12. Buzsáki, G., Penttonen, M., Nádasdy, Z. & Bragin, A. Pattern and inhibition-dependent invasion of pyramidal cell dendrites by fast spikes in the hippocampus *in vivo*. *Proc. Natl Acad. Sci. USA* **93,** 9921–9925 (1996).
13. Tsubokawa, H. & Ross, W. N. IPSPs modulate spike backpropagation and associated $[Ca^{2+}]_i$ changes in the dendrites of hippocampal CA1 pyramidal neurons. *J. Neurophys.* **76,** 2896–906 (1996).
14. Chen, H. & Lambert, N. A. Inhibition of dendritic calcium influx by activation of G-protein-coupled receptors in the hippocampus. *J. Neurophysiol.* **78,** 3484–3488 (1997).
15. Singer, W. & Gray, C. M. Visual feature integration and the temporal correlation hypothesis. *Annu. Rev. Neurosci.* **18,** 555–586 (1995).
16. Llinás, R., Ribary, U., Joliot, M. & Wang, X.-J. in *Temporal Coding in the Brain* (eds Buzsáki, G. *et al.*) 251–272 (Springer, Berlin, 1994).
17. Heilman, K. M. & Valenstein, E. *Clinical Neuropsycology* (Oxford Univ. Press, New York, 1993).
18. Cauller, L. J. & Kulics, A. T. The neural basis of the behaviorally relevant N1 component of the somatosensory-evoked potential in SI cortex of awake monkeys: evidence that backward cortical projections signal conscious touch sensation. *Exp. Brain Res.* **84,** 607–618 (1991).
19. Zhu, J. J. & Sakmann, B. Whisker-evoked slow oscillation (7–12 Hz) in single neurons of the rat barrel cortex. *Soc. Neurosci. Abstr.* **24,** 1512 (1998).
20. Zhu, J. J. & Connors, B. W. Intrinsic firing patterns and whisker-evoked synaptic responses of neurons in the rat barrel cortex. *J. Neurophysiol.* **81,** 1171–1183 (1999).
21. Lisman, J. E. Bursts as a unit of neural information: making unreliable synapses reliable. *Trends Neurosci.* **20,** 38–43 (1997).
22. Dodt, H. U. Infrared-interference videomicroscopy of living brain slices. *Adv. Exp. Med. Biol.* **333,** 245–249 (1993).

Acknowledgements. We thank B. Katz, A. Korngreen, G. Borst and A. Silver for their helpful comments. M.E.L. was supported by an Alexander von Humboldt scholarship and J.J.Z. was supported by a Max-Planck Gesellschaft fellowship.

Correspondence and requests for materials should be addressed to M.E.L. (e-mail: mlarkum@sunny.mpimf-heidelberg.mpg.de).

Signalling through CD30 protects against autoimmune diabetes mediated by CD8 T cells

Christian Kurts*, Francis R. Carbone†, Matthew F. Krummel‡, Karl M. Koch*, Jacques F. A. P. Miller‡ & William R. Heath‡

** The Department of Nephrology, Medizinische Hochschule, 30625 Hannover, Germany*

† The Department of Pathology and Immunology, Monash Medical School, Prahran, Victoria 3181, Australia

‡ The Immunology Division, The Walter and Eliza Hall Institute of Medical Research, Parkville, Victoria 3050, Australia

Autoantigens found on pancreatic islets can move to draining lymph nodes, where they are able to cause the activation and consequent deletion of autoreactive T cells by a mechanism termed cross-tolerance[1,2]. This deletion depends on signalling through CD95 (also known as Fas), a member of the superfamily of tumour-necrosis-factor receptors[3]. Here we describe a new mechanism that protects against autoimmunity: this mechanism involves another member of this superfamily, CD30, whose function was largely unknown. CD30-deficient islet-specific CD8-positive T cells are roughly 6,000-fold more autoaggressive than wild-type cells, with the transfer of as few as 160 CD30-deficient T cells leading to the complete destruction of pancreatic islets and the rapid onset of diabetes. We show that, in the absence of CD30 signalling, cells activated but not yet deleted by the CD95-dependent cross-tolerance mechanism gain the ability to proliferate extensively upon secondary encounter with antigen on parenchymal tissues, such as the pancreatic islets. Thus, CD30 signalling limits the proliferative potential of autoreactive CD8 effector T cells and protects the body against autoimmunity.

CD30 is a member of the tumour-necrosis-factor receptor (TNFR) superfamily, and is expressed by activated, but not by resting, B or T cells[4–8]. Although its function is largely unknown, *in vitro* studies have shown that it has effects on both cell death and cell activation[7–11]. T cells of the T-helper-2 phenotype may express CD30 (ref. 6), although this has been questioned[12]. Mice deficient in CD30 showed a mild impairment in thymic negative selection[13], but a function for CD30 in the *in vivo* response of mature T cells has yet to be demonstrated.

Here we investigated the role of CD30 signalling in the maintenance of self-tolerance by using a model system in which ovalbumin (OVA)-specific $CD8^+$ T cells from the OT-I transgenic line (OT-I cells) were adoptively transferred into unirradiated transgenic mice that expressed OVA in the pancreatic β-cells and the proximal tubular cells of the kidney (RIP-mOVA mice)[14]. In this model, wild-type OT-I cells caused diabetes only when adoptively transferred in relatively large numbers (>250,000 cells) (Table 1), with lower doses being effectively tolerized. In contrast, CD30-deficient OT-I cells (OT-I.$CD30^{-/-}$ cells) were highly diabetogenic, with as few as 160 cells causing disease. The diabetogenic potential of such small doses of CD30-deficient cells indicates that CD30 is important in the prevention of autoimmunity mediated by $CD8^+$ T cells.

We have shown previously that OT-I cells are slowly deleted by a CD95-dependent mechanism in the weeks following transfer into RIP-mOVA mice[3]. CD30 deficiency did not impair this slow deletion process (data not shown), but seemed to exert its effect much earlier than did CD95, as indicated by the rapid onset of diabetes as early as 4 days after adoptive transfer. To gain understanding of what was happening in these few days following adoptive transfer, we used flow cytometry to count wild-type and CD30-deficient OT-I cells in the spleen and lymph nodes of RIP-mOVA mice shortly after adoptive transfer (Fig. 1). There was a marked antigen-specific increase (expansion) in the number of CD30-deficient cells, but not of wild-type OT-I cells, peaking on days 4–5 after adoptive transfer into RIP-mOVA mice. This expansion was accompanied by prominent infiltration of the CD30-deficient cells into the pancreas and by β-cell destruction (data not shown). Thus, CD30-deficient cells

Table 1 CD30-deficient OT-I cells cause diabetes in RIP-mOVA mice

No. of injected cells	No. of diabetic mice/no. in group	
	OT-I	OT-I.$CD30^{-/-}$
5,000,000	18/18	5/5
2,000,000	9/10	9/9
1,000,000	4/8	6/6
250,000	0/26	9/10
100,000	0/7	9/11
20,000		12/13
4,000		6/6
800		9/13
160		4/9

Data from several experiments are pooled. Mice were injected with semi-purified OT-I or OT-I.$CD30^{-/-}$ T cells and then examined for diabetes by analysis of urine glucose as described[15]. In some experiments, diabetes was confirmed by analysis of blood glucose, and islet destruction was confirmed by histology as described[15]. Diabetes onset occurred between days 4 and 10, depending on the number of cells transferred.